ASRL TR 143-1

VORTEX WAKE ROLLUP AND VORTICITY CONCENTRATION BEHIND AN AIRFOIL

Thomas Arthur McMahon
and
Sheila Evans Widnall

MASSACHUSETTS INSTITUTE OF TECHNOLOGY
AEROELASTIC AND STRUCTURES RESEARCH LABORATORY

June 1967

UNITED STATES ARMY RESEARCH OFFICE
DURHAM
CONTRACT NO. DA-31-124-ARO-D-471

ASRL TR 143-1

VORTEX WAKE ROLLUP AND VORTICITY CONCENTRATION BEHIND AN AIRFOIL

Thomas Arthur McMahon
and
Sheila Evans Widnall

MASSACHUSETTS INSTITUTE OF TECHNOLOGY
AEROELASTIC AND STRUCTURES RESEARCH LABORATORY

June 1967

UNITED STATES ARMY RESEARCH OFFICE
DURHAM
CONTRACT NO. DA-31-124-ARO-D-471

ABSTRACT

Some important experimental evidence seems to confirm that the near wake problem is basically three-dimensional and should be reexamined as such. A concentration mechanism based on this three-dimensionality is proposed and found to predict a gradient of core circulation which is dimensionally correct and gives realistic answers when specific numerical cases are compared to published experiments. The correlation of experiment with theory involves a uniform translation of the theoretical points a specific distance upstream, implying that rotational fluid in the sheet requires a finite, uniform time to get to the core, no matter which downstream station we consider. A paradox in the role of viscosity in the concentrating mechanism is discussed.

TABLE OF CONTENTS

SYMBOLS

r, θ, z	Coordinate directions (Fig. 3)
u, v, w	Velocity component in r, θ, z directions
W	Free-stream velocity in "region adjacent to vortex core"
ρ	Fluid density (constant)
ν	Kinematic viscosity
Γ_c	Circulation around the vortex core
R	Vortex core radius
γ_c	Local vorticity in the core
γ_s	Local vorticity in the vortex sheet, accommodated to axial symmetry
D_o	Drag of a vortex-producing body
t	Time, seconds

SECTION I

THE MOTION OF A VISCOUS VORTEX IN THE PRESENCE OF A VORTEX SHEET

Reference 3, a companion publication written concurrently with the present report, reviews several analytical approaches to the vortex sheet rollup problem. All of these which treat the motion as two-dimensional appear to be partially unrealistic in the face of the observed "tightening" or concentration of vorticity in the vortex core. An explanation for this observed concentration of vorticity in the core must come from a recognition of the basic three-dimensional character of the flow, where one mechanism (though perhaps not the only one) for the transport of vorticity from the region of the sheet to the region of the core is the local divergence of the stream tubes which make up the core.

A model for the vorticity concentrating mechanism is proposed to be the following:

Figure 2 represents a three-quarter view of the geometry of the rolling up process. The core region is a quasi-cylinder of rotational fluid whose interior may contain axial (in the z direction) velocities which may be responsible for local stretching or compression of the core. Wrapping the core region is a blanket of irrotational fluid which we shall hereafter call "Fluid Adjacent to the Core," which can flow into the core under the action of local divergence of the core stream tubes. Notice that the core envelope, which was defined as the locus of points in space where the tangential induced velocity was numerically a maximum, is <u>not</u> a stream tube. If the core envelope <u>were</u> a stream tube, it would not be possible for fluid in the vortex sheet to be convected into the vortex core, violating the consensus of above-mentioned experimental observations which indicate that

this convection does take place.

From mass conservation,

$$-2\pi R(z)\bar{u}(z)dz = \left(\pi R^2 \frac{\partial \bar{w}}{\partial z} + 2\pi R \bar{w} \frac{\partial R}{\partial z}\right) dz \qquad (1.1)$$

Here R(z) denotes the radius of the vortex core, $\bar{u}(z)$ is the azimuth-averaged radial velocity at z drawing fluid into the core, and $\bar{w}(z)$ is the axial velocity averaged over the cross-sectional area of the vortex core.

Suppose that both the geometry of the core envelope and the entire three-dimensional flow u,v,w of r,θ,z were specified. Then purely geometric considerations would determine how vorticity-bearing fluid crossed the core envelope:

$$W \frac{\partial \Gamma_c}{\partial z} = \gamma_s \left[-\bar{u}(z) + W \frac{\partial R}{\partial z}\right] 2\pi R(z) \qquad (1.2)$$

The above relation is visually verified by observing that an element of core wall surface may be projected either on a plane orthogonal to the u or w component of velocity. The sum of these two effects gives the net rate at which vorticity-bearing fluid crosses the core wall. The left side of the equation contains the free stream velocity W because, in this three-dimensional steady problem, downstream distance replaces time as the variable to which rates of accumulation are referenced. Combining (1.1) and (1.2),

$$\frac{\partial \Gamma_c}{\partial z} = \frac{\gamma_s}{W}\left[\frac{R}{2}\frac{\partial \bar{w}}{\partial z} + \bar{w}\frac{\partial R}{\partial z} + W\frac{\partial R}{\partial z}\right] 2\pi R(z) \qquad (1.3)$$

Batchelor, Ref. 1, has shown that a viscous laminar swirling flow which is probably descriptive of the motion in a trailing wing-tip vortex far downstream is given by:

$$\Gamma = \Gamma_0 \left(1 - e^{-\frac{W r^2}{4\nu z}}\right) \tag{1.4}$$

This similarity solution is not strictly valid in the region we are considering for the following reasons:

i) The solution was derived assuming that the axial velocity w is nearly equal to the free stream velocity W, a linearization which removes terms from the momentum equations which describe the "vortex stretching" aspect of the motion, i.e. the transport of tangential momentum caused by vortical fluid moving from a greater to a smaller radius.

ii) The equations from which the solution was derived are descriptive of laminar flow; yet it is almost certain that the flow behind real airfoils in the rollup regime is turbulent.

In spite of the above reservations, the similarity solution (1.4) is a useful first guess for the actual flow in a rolling up vortex core. When we use (1.3) to calculate the axial gradient of core circulation, you recall that we only needed to know how $\bar{w}$, axial velocity defect averaged over a cross-section, varies with downstream distance z. The equations of motion for steady axisymmetric flow of incompressible fluid were, without approximation:

$$w \frac{\partial w}{\partial z} + v \frac{\partial w}{\partial r} = -\frac{1}{\rho} \frac{\partial p}{\partial z} + \nu \nabla^2 w \tag{1.5}$$

$$w \frac{\partial v}{\partial z} + v \frac{\partial v}{\partial r} - \frac{v^2}{r} = -\frac{1}{\rho} \frac{\partial p}{\partial r} + \nu \left(\nabla^2 v - \frac{v}{r^2}\right) \tag{1.6}$$

$$w\frac{\partial v}{\partial z} + u\frac{\partial v}{\partial r} + \frac{uv}{r} = \nu\left(\nabla^2 v - \frac{v}{r^2}\right) \tag{1.7}$$

where

$$\nabla^2 = \frac{\partial^2}{\partial z^2} + \frac{\partial^2}{\partial r^2} + \frac{1}{r}\frac{\partial}{\partial r}$$

In deriving the similarity form (1.4) interest is usually restricted to flows where axial gradients are of small magnitude compared with radial gradients. Thus, the approximations

$$\frac{\partial}{\partial z} \ll \frac{\partial}{\partial r} \tag{1.8}$$

and

$$u \ll w \tag{1.9}$$

are introduced into the above, and now

$$\nabla^2 = \frac{\partial^2}{\partial r^2} + \frac{1}{r}\frac{\partial}{\partial r} \tag{1.10}$$

in Eqs. (1.5) and (1.6).

If the further linearization

$$|w - W| \ll W \tag{1.11}$$

strictly valid only in the far downstream regime, is made, Eq. (1.5) reduces to:

$$W\frac{\partial w}{\partial z} = -\frac{1}{\rho}\frac{dp}{dz} + \nu\left(\frac{\partial^2 w}{\partial r^2} + \frac{1}{r}\frac{\partial w}{\partial r}\right) \tag{1.12}$$

and (1.6) becomes

$$\frac{1}{\rho}\frac{\partial p}{\partial r} = \frac{v^2}{r} \tag{1.6a}$$

while (1.7) becomes

$$W\frac{\partial v}{\partial z} = \nu\left(\frac{\partial^2 v}{\partial r^2} + \frac{1}{r}\frac{\partial v}{\partial r} - \frac{v}{r^2}\right) \tag{1.13}$$

Equation (1.13) is identically the relation describing viscous decay of circulating motion in two dimensions when τ is replaced by z/W. Therefore, we derive the form (1.4) as a solution to (1.13) strictly valid only for large z. As we mentioned earlier, there is an additional reason why (1.13) isn't descriptive of the actual rollup motion: the $u\frac{\partial v}{\partial r}$ term in Eq. (1.7) has dropped out, and it is precisely this term which describes the "vortex stretching" motion, the "spin up" caused by an inward transport of tangential momentum. It is regretable that the inclusion of this term renders the problem unsuitable to a similarity solution, for the present analysis depends on such a solution to proceed any farther.

Supposing the pressure far from the axis of the vortex to be uniform, we integrate (1.6a)

$$\frac{p_0 - p}{\rho} = \int_r^\infty \frac{\Gamma^2(r)}{4\pi^2 r^3}\,dr \tag{1.14}$$

and substitute this into (1.12)

$$W\frac{\partial w}{\partial z} - \nu\left(\frac{\partial^2 w}{\partial r^2} + \frac{1}{r}\frac{\partial w}{\partial r}\right) = \frac{1}{4\pi^2}\int_r^\infty \frac{1}{r^3}\frac{\partial \Gamma^2}{\partial z}\,dr = \frac{2\nu}{4\pi^2 W}\int_r^\infty \frac{\Gamma}{r^2}\frac{\partial}{\partial r}\left(\frac{1}{r}\frac{\partial \Gamma}{\partial r}\right)dr \tag{1.15}$$

substituting (1.4) into (1.14)

$$\frac{p_0 - p}{\rho} = \frac{\Gamma_0^2 W}{4\pi^2 \nu z}\,P(\eta) \tag{1.16}$$

where

$$P(\eta) = \int_\eta^\infty \frac{(1 - e^{-\xi})^2}{\xi^2}\,d\xi$$

$$= \frac{(1 - e^{-\eta})^2}{\eta} + 2ei(\eta) - 2ei(2\eta)$$

and:

$$ei(\eta) = \int_\eta^\infty \frac{e^{-\xi}}{\xi}\,d\xi$$

Now (1.15) becomes:

$$W\frac{\partial w}{\partial z} - \nu\left(\frac{\partial^2 w}{\partial r^2} + \frac{1}{r}\frac{\partial w}{\partial r}\right) = -\frac{\Gamma_0^2 W}{4\pi^2 8\nu Z^2}\left(P(\eta) + \eta\frac{dP}{d\eta}\right) \tag{1.17}$$

At last the simplification which arises from chosing the similarity form (1.4) to be representative of the flow in the rollup region becomes apparent. For if we integrate (1.17) over any cross-sectional plane, we find the terms multiplying ν integrate to zero.

$$W\frac{d}{dz}\int_0^\infty w(r)r\,dr - \nu\int_0^\infty\left[\frac{\partial^2 w}{\partial r^2}r + \frac{\partial w}{\partial r}\right]dr = \int_0^\infty -\frac{\Gamma_0^2 W}{4\pi^2 8\nu Z^2}\frac{d(\eta P)}{d\eta}r\,dr \tag{1.18}$$

$$W\frac{d}{dz}\int_0^\infty w(r)r\,dr - \nu\int_0^\infty \frac{d\left(r\frac{\partial w}{\partial r}\right)}{dr}\,dr = -\frac{\Gamma_0^2 W 4\nu Z}{4\pi^2 8\nu Z^2 Z W}\left[\eta P\right]_0^\infty$$

$$W\frac{d}{dz}\int_0^\infty w(r)r\,dr - \nu\left[r\frac{\partial w}{\partial r}\right]_0^\infty = -\frac{\Gamma_0^2}{16\pi^2 Z}\left[\eta P\right]_0^\infty$$

Evaluating the limits, we see that since $\frac{\partial w}{\partial r} \to 0$ as $r \to \infty$, and since $P \to \eta^{-1}$ as $\eta \to \infty$,

$$-\frac{d}{dz}\int_0^\infty w(r)r\,dr = \frac{\Gamma_0^2}{16\pi^2 WZ} \tag{1.19}$$

and finally, since adding an arbitrary constant to w in the integrand on the left side of the equation will make no difference at all whenever the gradient with respect to z comes to be applied,

$$\frac{d}{dz}\int_0^\infty (W - w)r\,dr = \frac{\left(\frac{\Gamma_0}{2\pi}\right)^2}{4WZ} \tag{1.20}$$

Equation (1.20) exhibits the remarkable feature of being independent of viscosity. All the terms multiplying the viscosity in the equations of motion have integrated to zero, showing that the effect of viscosity behind a wing is to produce a "spreading" of the axial velocity defect, without producing a change in the total magnitude of the defect.

Dividing both sides of (1.20) by the cross-sectional core area, πR^2, we obtain the dependence of averaged axial velocity gradient on total circulation for this particular swirling flow:

$$\frac{d\bar{w}}{dz} = \frac{1}{\pi R^2}\frac{d}{dz}\int_0^\infty (W-w)\,r\,dr = \frac{\left(\frac{\Gamma_0}{2\pi}\right)^2}{4\pi R^2 W z} \qquad (1.21)$$

Substituting (1.21) into (1.3), we discover the relation which predicts the extent to which this particular swirling flow, in the neighborhood of a vortex sheet of local strength γ_s, concentrates vorticity in its core:

$$\frac{d\Gamma_c}{dz} = \frac{\gamma_s 2\pi R R\left(\frac{\Gamma_0}{2\pi}\right)^2}{4\cdot 2R^2W^2Z} + \frac{\partial R}{\partial z}(\bar{w}+W)\frac{\gamma_s}{W}2\pi R(z) \qquad (1.22)$$

If we suppose $\bar{w}$ to be sufficiently like W in the roll-up region so that $\bar{w}\sim W$ and

$$\frac{\bar{w}+W}{W} \simeq 2 \qquad (1.23)$$

then:

$$\frac{d\Gamma_c}{dz} = \frac{\gamma_s\,\Gamma_c^2(z)}{W^2 16\pi^2 z} + \frac{\partial R}{\partial z}\gamma_s 4\pi R(z) \qquad (1.24)$$

Equation (1.24) represents the goal of our analysis. Given the "state" of any rolling up vortex system, i.e. given the free stream velocity, core radius and downstream gradient of core radius, sheet vorticity, and local circulation, (1.24) predicts how fast sheet vorticity is being concentrated in the core region. It may seem paradoxical that kinematic viscosity does not appear as a parameter even though the model

depends on viscous effects to do the concentrating. This contradiction is quickly dismissed by the observation that each of the parameters which does appear in (1.24) is implicitly dependent on viscosity, and each would have a different dependence on the downstream coordinate z if kinematic viscosity were changed.

SECTION II

COMPARISON WITH A PUBLISHED EXPERIMENT

Recently, in a paper published by the Pennsylvania State University Department of Aeronautical Engineering, B. W. McCormick and J. L. Tangler, Ref. 2, have reported on their measurements of the local angular velocity in a vortex sheet immediately behind an aircraft wing in flight. Using a vorticity meter which was essentially an infinite-pitched free propeller, contour maps of constant rotational speed were plotted for several planes orthogonal to the flight direction downstream of an aircraft wing. Those for a typical flight speed, W=75 MPH, are reproduced in Figs. 3 and 4.

Certain difficulties were encountered in making these measurements which we would do well to consider. While the data were being taken, the necessity of holding the aircraft on a straight and level course required control movements which changed the position of the vortex probe relative to the vortex sheet. These disturbances, which were amplified as the vortex probe moved downstream, made interpretation of the data difficult. In fact, the configuration of vorticity distributions more than three feet downstream was open to doubt; and many data points had to be interpreted in the combined knowledge of similar points fore and aft of those being considered. Experiments were also performed with a scale model of the actual aircraft wing in a wind tunnel, and these were useful in interpreting the in-flight data. No correction was applied to the data of Figs. 3 and 4 for the calibration of the vortex probe, nor for the fact that the probe had a finite size (vane diameter 3/4 inches). The contour maps were measured at a variety of different altitudes between 5000 and 9000 feet, but a comparison of a particular plot for

the same indicated airspeed at two extremes of altitude showed the total circulation was less than 4% different between the two cases, and therefore differences in density altitude were deemed to be unimportant for the experiment.

Even though the above-cited work can be expected to contain some imprecision because of these difficulties, it is, nevertheless, a remarkable achievement, being the only vorticity mapping behind an aircraft in flight now available. Starting with Figs. 3 and 4, we shall reduce the data to be consistent with the radial symmetry of our model and determine whether our solution (1.24) predicts realistic values of vortex sheet strength when the other parameters in (1.24) are taken from experiment. The reader realizes that this is only one way in which an experimental corroboration of (1.24) could be obtained; but as we proceed, it may become evident why this choice is the logical one.

Figures 3 and 4 were replotted on 10x10 to the centimeter graph paper, and the areas of each of the irregular concentric regions bounded by contour lines of constant angular velocity were tabulated by counting the number of squares enclosed. These areas were recorded in the column labeled A_i in Table I. The angular velocity of the fluid in each area A_i was taken to be the average between the two enclosing lines of constant angular velocity, and this is recorded in the next column of Table I under the heading Ω_i. An equivalent circularized radius for each of the irregular areas A_i is found by the formula:

$$R_i = \sqrt{\frac{A_1 + A_2 + \cdots A_i}{\pi}} \qquad (2.1)$$

and recorded in the next column. Finally, the tangential velocity appropriate to each circularized radius is found

from an application of Stokes' theorem:

$$V_i = \frac{2\pi \cdot 2}{2\pi \cdot 60} \quad \frac{1}{R_i} \left(\Omega_1 A_1 + \Omega_2 A_2 + \cdots \Omega_i A_i \right) \qquad (2.2)$$

Figure 5 presents a plot of tangential velocity plotted against radial distance for each of the six downstream planes sampled. It is apparent that the one, two, and three foot downstream stations exhibit velocity profiles which have well-defined maxima, but that subsequent profiles grow progressively broader until a local maximum can no longer be discerned. The radial coordinate of the maximum of each curve is arbitrarily designated the radius of the vortex core at that particular downstream station. This is not to imply that no rotational fluid exists outside of this radius; Figs. 3 and 4 confirm that measurable fluid rotation exists at radii greater than what we call the radius of the vortex core in nearly every contour plot. But since the vortex wake rollup system is a fluid flow which has rotational character both near and far from the axis of the core, (i.e. the core region itself and the vortex sheet), and since the mechanism explained in Section III requires only that the core radius be defined as some radial locus of points easily discernable from others, and since it is desirable to include as much of the core rotation as practical in the core region, we put all these requirements together and name the locus of the maximum of the tangential velocity curve as the core radius. We could, for example, have chosen a constant-radius cylinder as the locus of the core radius; but this choice might have prevented our discovering whether or not vorticity concentration proceeds independently of how large you make the radius of that cylinder. That is, one can imagine a cylinder so large that only the motion of the most remote sections of the vortex sheet enters into the question of how

rapidly vorticity is being concentrated in the core, or perhaps a cylinder so small and therefore so close to the vortex axis that we are really talking about a vortex microcore which may not be representative of the whole core at all. Our actual choice appears to be a compromise of these extremes.

Having decided what the radius of the core is for all of the six downstream stations, we plot these versus downstream distance in Fig. 6 . From the curve, we tabulate the gradient of core size in the downstream direction. It is apparent that for our definition of core size, the core narrows slightly immediately downstream, but then grows fairly linearly with distance after that. In Table II, the total circulation strength of the rotational fluid enclosed inside the above-defined core radius is computed, again by an application of Stokes' theorem. This is plotted against downstream distance in Fig. 7 and the best segmented straight line is fitted. The slopes of the straight line segments in Fig. 7 are tabulated in Table III, as are the other parameters discussed earlier which we said characterized the state of the flow field. The formula (1.24) is applied to each flow state to obtain a prediction for γ_s , the angular velocity of the "fluid immediately adjacent to the vortex core" which we suppose to have originally started in the vortex sheet. The result of this computation for each downstream station is plotted in Fig. 8 , along with a shaded band which represents the upper and lower limits of rotational strength of fluid present in the region of the vortex sheet. One may see that the data points lie quite strictly parallel to, but not in the range of, the band representing sheet rotation. If one imagines that a finite, specified time interval elapses between the time when a rotational fluid particle is in the sheet region and the time when it arrives in the "region adjacent to the core" preparatory to being ingested into the

core, one sees that an appropriate comparison between the theoretical points and the experimental band involves a uniform translation of all the points to the left in the figure. It is not possible to say exactly how much this translation should be, because the precise path which the rotational particles take from the sheet to the core, and the time required to traverse this path, is not well understood. It is only clear that such a transfer does take place, as documented in Ref. 2, and that it does take a finite amount of time, and this time is probably quite similar whether we first started tracking the particle in the sheet one foot downstream or three feet downstream. Since, if all the computed points were translated to the left, i.e. compared to the experimental band a uniform distance upstream in every case, the computed points could be made to lie quite well within the experimental band, we claim that the theory presented in Section I is able to predict the results of experiments very capably. Incorporated in this judgment is an appreciation of the difficulties under which the experimental work was done, the confessed naivete of our omission from the similarity problem of the vortex stretching or "spin-up" terms, and the errors and varience contributed by our forcing the contour plots into radial symmetry. Even with these random effects operating, the comparison we suggest in Fig. 8 seems believable. One might even have guessed that the computed points must lie to the left of the experimental band: in fact, if it weren't for this feature, the conclusion would have to be that vortex filaments move from the sheet to the region adjacent to the vortex core in zero time, an absurd suggestion.

SECTION III

SUMMARY

A knowledge of how the vortex sheet trailing an airfoil rolls up into a single trailing vortex is particularly important to rotary wing aerodynamic theory.

Experimental observations indicate that vorticity is concentrated in the rolling-up vortex core. Existing theoretical techniques of analysis, including selfsimilar hydrodynamics, vortex system theory, conservation of energy arguments, and others are not able to account for this observed concentration of vorticity in the core because they treat the motion as two-dimensional.

A concentration mechanism is proposed whereby the three-dimensional, viscous nature of flow in the core draws rotational fluid inward as a consequence of the local divergence of stream tubes in the core. The analysis includes an integration over the entire radial coordinate, and may therefore be called an integral technique because it is only able to predict whether or not vorticity is concentrated in the core region when a particular swirling flow is specified. A classical three-dimensional viscous vortex similarity solution is taken to represent the actual flow in the core and is substituted into the integral formulation. When this is done, the final result predicting circulation gradient in the core exhibits the remarkable feature of being not explicitly dependent on viscosity, although other parameters specifying the circulation gradient do depend on viscosity. An implication of this result is that viscosity acts to control the spreading of vorticity in the radial direction, but does not actually create vorticity in the wake.

When a set of data derived from published experiments involving an in-flight mapping of the vortex wake behind an aircraft wing are compared to the above theory, a correlation results which is particularly satisfactory because it implies that a finite time elapses between the time when a certain vortical fluid element is observed in the sheet and the time when it is observed at the edge of the core. This finite time is relatively uniform between the various downstream stations, indicating that inflow into the core proceeds at a relatively constant rate, consistent with other deductions from the experiment. On the basis of this and other successful experimental comparisons, the concentration mechanism proposed is claimed to be credible within the tolerances of experimental variances and the simplicity of the model.

REFERENCES

1. Batchelor, G. K., "Axial Flow in Trailing Line Vortices," Journal of Fluid Mechanics, Vol. 20, p. 654, Dec. 1964.

2. McCormick, B. W., and Tangler, J. L., A Study of the Vortex Sheet Immediately Behind an Aircraft Wing, Aero. Engineering Report, Pennsylvania State, December 1965.

3. McMahon, T. A., Review of the Vortex Rollup Problem, June 1967, ASRL TR 145-1.

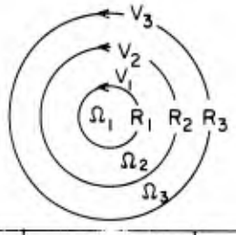

DOWNSTREAM DISTANCE	i	A_i IN^2	$\frac{\Omega_1}{10^3/60}$ $\frac{REV}{SEC}$	$R_i = \frac{A_1 + \cdots A_i}{\pi}$ IN.	$V_i = \frac{2\pi \cdot 2}{60} (\Omega_1 A_1 + \Omega_2 A_2 + \cdots \Omega_1 A_1) \frac{1}{R_i}$ IN/SEC
12 IN.	1	.81	$\frac{6.6+6.0}{2} = 6.3$	0.51	(5.2)(.035)/.51 = 330
	2	4.9	$\frac{6.0+3.0}{2} = 4.5$	1.35	(5.2 + 22.0)(.035)/1.35 = 690
	3	9.5	$\frac{3.0+0.6}{2} = 1.8$	2.20	(5.2 + 22.0 + 17.1)(.035)/2.20 = 660
24 IN.	1	0.75	$\frac{9.0+6.0}{2} = 7.5$	0.49	(5.6)(.035)/.49 = 370
	2	2.55	$\frac{6.0+3.0}{2} = 4.5$	1.03	(5.6 + 11.5)(.035)/1.03 = 550
	3	15.9	$\frac{3.0+0.6}{2} = 1.8$	2.49	(5.6 + 11.5 + 28.6)(.035)/2.49 = 600
36 IN.	1	2.37	$\frac{8.7+6.0}{2} = 7.3$	0.87	(17.3)(.035)/.87 = 640
	2	8.24	$\frac{6.0+3.0}{2} = 4.5$	1.84	(17.3 + 37.1)(.035)/1.84 = 970
	3	9.30	$\frac{3.0+0.6}{2} = 1.8$	2.70	(17.3 + 37.1 + 16.7)(.035)/2.70 = 860
48 IN.	1	1.87	$\frac{8.7+6.0}{2} = 7.3$	0.77	(13.6)(.035)/.77 = 580
	2	6.3	$\frac{6.0+3.0}{2} = 4.5$	1.61	(13.6 + 28.4)(.035)/1.61 = 860
	3	17.4	$\frac{3.0+0.6}{2} = 1.8$	2.97	(13.6 + 28.4 + 31.3)(.035)/2.85 = 840
60 IN.	1	2.0	$\frac{10.2+6.0}{2} = 8.1$	0.80	(16.2)(.035)/.80 = 660
	2	6.1	$\frac{6.0+3.0}{2} = 4.5$	1.60	(16.2 + 27.5)(.035)/1.60 = 920
	3	19.7	$\frac{3.0+0.6}{2} = 1.8$	2.97	(16.2 + 27.5 + 35.5)(.035)/2.97 = 890
72 IN.	1	1.56	$\frac{8.4+6.0}{2} = 7.2$	0.70	(11.2)(.035)/.70 = 520
	2	5.37	$\frac{6.0+3.0}{2} = 4.5$	1.59	(11.2 + 23.3)(.035)/1.59 = 710
	3	27.50	$\frac{3.0+0.6}{2} = 1.8$	3.36	(11.2 + 23.3 + 49.5)(.035)/3.36 = 820

TABLE I : REDUCING THE CORE TO RADIAL SYMMETRY

DOWNSTREAM DISTANCE, INCHES	CORE RADIUS INCHES	CORE STRENGTH, IN^2/SEC
12	1.7	$(10^3).21[5.2 + 22.0 + 6.0] = 7.0 \times 10^3$
24	1.62	$(10^3).21[5.6 + 11.5 + 8.5] = 5.4 \times 10^3$
36	1.75	$(10^3).21[17.3 + 32.5] = 10.5 \times 10^3$
48	2.25	$(10^3).21[13.6 + 28.4 + 13.$ [illegible] $= 11.7 \times 10^3$
60	2.25	$(10^3).21[16.2 + 27.5 + 13.9$ [illegible] $= 12.1 \times 10^3$
72	3.36	$(10^3).21[11.2 + 25.0 + 49.5] = 18.0 \times 10^3$

$$\Gamma_c = 10^3 \cdot \frac{2\pi \cdot 2}{60} \cdot \left[A_1 \Omega_1 + A_2 \Omega_2 + \cdots \Omega_j \pi (R_n^2 - R_{j-1}^2)\right]$$

$[\ ]_n$ = DOWNSTREAM DISTANCE INDEX

$[\ ]_j$ = LARGEST RADIAL INDEX

TABLE II CORE STRENGTH COMPUTED

$$\frac{d\Gamma_c}{dz} = \left(\frac{\Gamma_o^2}{W^2\, 16\, \pi^2 z} + \frac{\partial R}{\partial Z}\, 2\pi R \right) \gamma_s$$

IN ALL BELOW,

$$W = 75 \text{ mph} = \frac{\overset{25}{\cancel{75}} \cdot 5.28 \cdot 10^{\cancel{3}} \cdot \cancel{12}}{\cancel{3}\cancel{60} \cdot \cancel{60}} = 1320 \text{ IN/SEC}$$

$$; W^2 = 1.74 \times 10^6 \text{ IN}^2/\text{SEC}^2$$

Γ_o, $\frac{IN^2}{SEC}$	Γ_o^2	Γ_o^2/W^2	Z	γ_s REV/MIN	γ_s RAD/SEC	$\frac{d\Gamma_c}{dZ}\frac{IN}{SEC}$	$\frac{dR}{dZ}$
7.0×10^3	4.9×10^7	2.83×10	12	$.64 \times 10^4$	1.34×10^3	-133	$-.6 \times 10^{-2}$
5.4×10^3	2.9×10^7	1.67×10	24	2.75×10^3	$.57 \times 10^3$	+415	1.1×10^{-2}
10.5×10^3	1.1×10^8	6.32×10	36	$.90 \times 10^3$	1.9×10^2	+133	3.4×10^{-2}
11.7×10^3	1.37×10^8	7.88×10	48	$.65 \times 10^3$	1.36×10^2	+ 40	3.4×10^{-2}
12.1×10^3	1.46×10^8	8.40×10	60	4.35×10^2	$.91 \times 10^2$	+610	3.4×10^{-2}

TABLE III SHEET STRENGTH COMPUTED

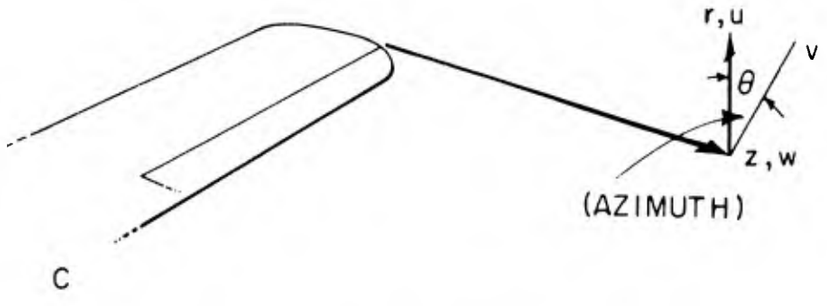

FIG. 1 COORDINATE SYSTEM

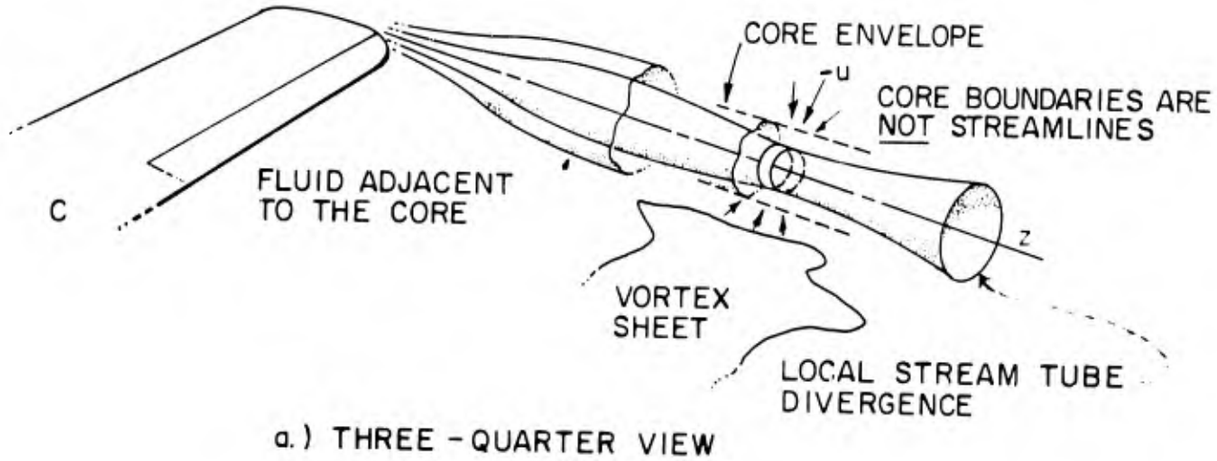

a.) THREE-QUARTER VIEW

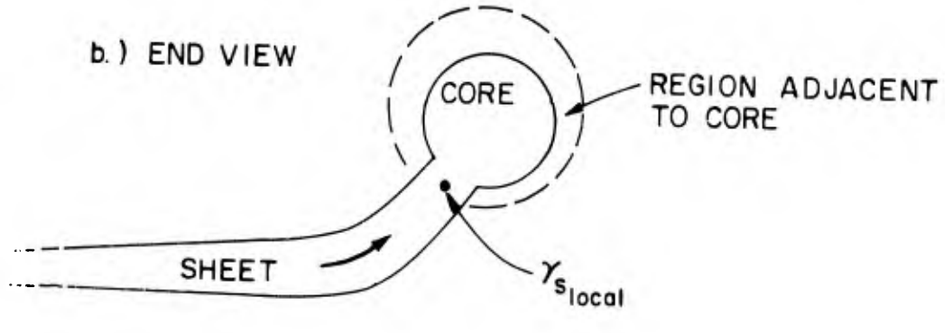

FIG. 2 LOCAL STREAM DIVERGENCE PRODUCING VORTICITY CONCENTRATION

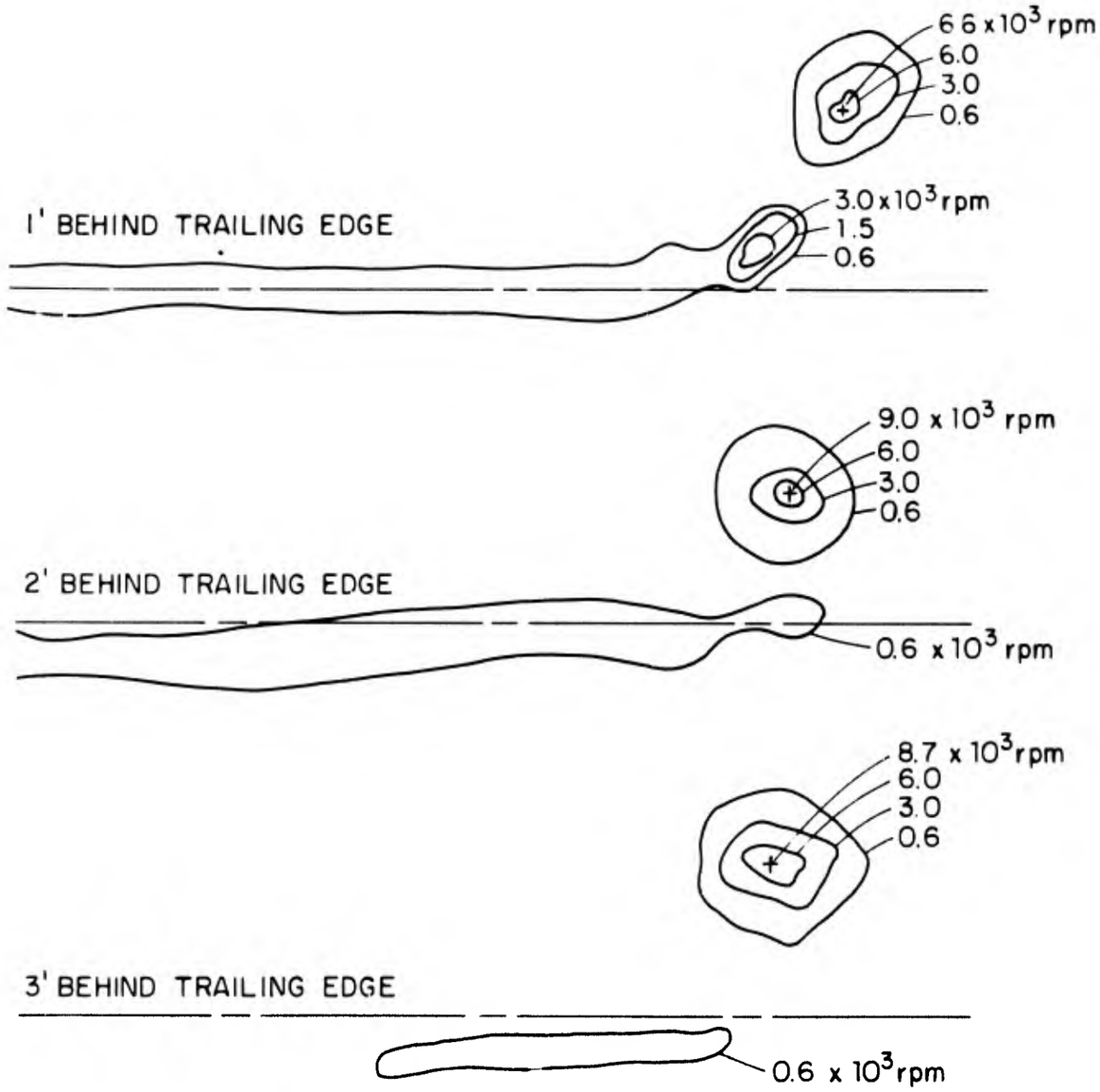

FIG. 3 FLIGHT DATA : CONTOURS OF CONSTANT ROTATIONAL SPEED, RPM

FLIGHT DATA : CONTOURS OF CONSTANT ROTATIONAL SPEED IN THREE TRANSVERSE PLANES DOWNSTREAM OF L-19 WING

W = 75 MPH

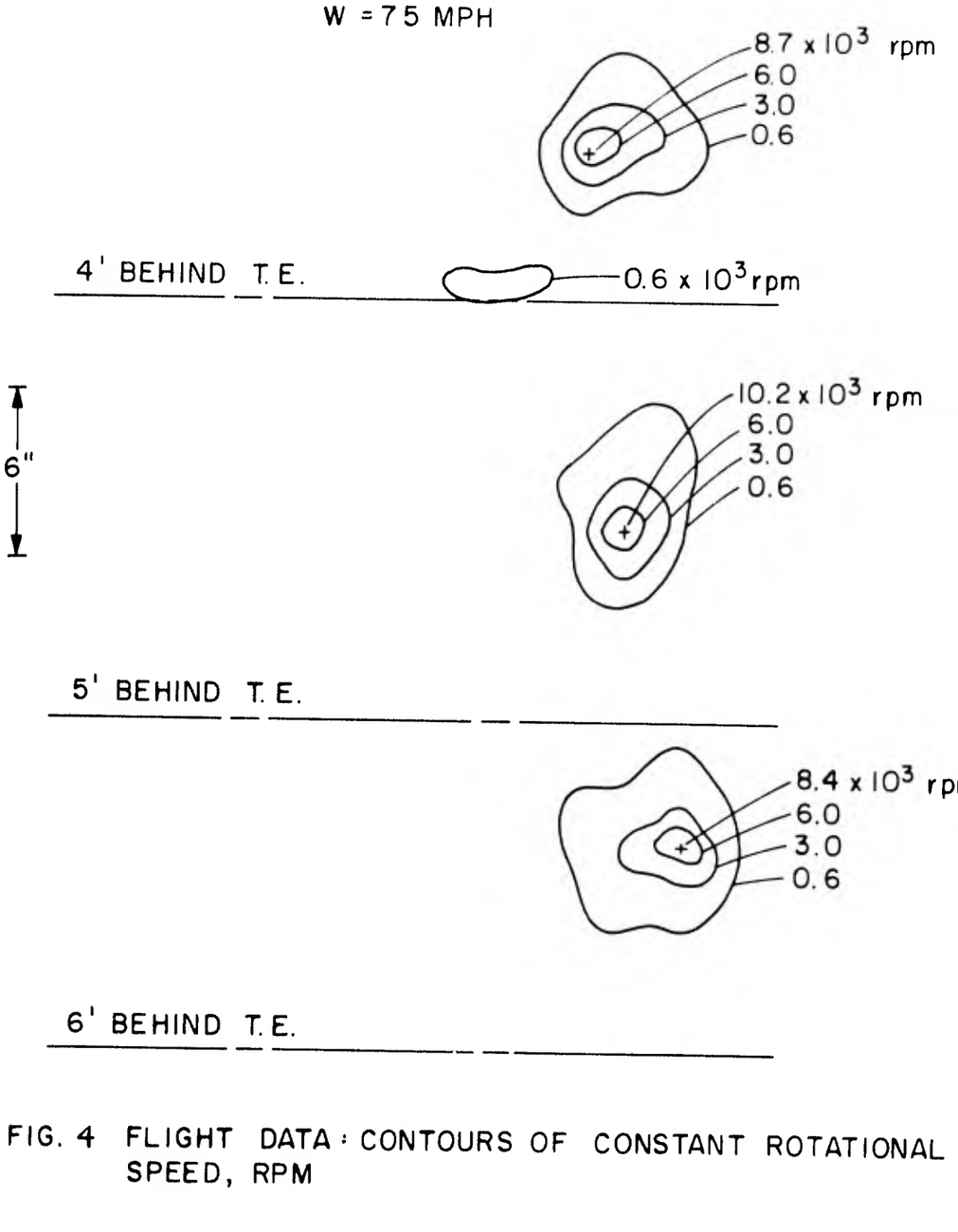

FIG. 4 FLIGHT DATA : CONTOURS OF CONSTANT ROTATIONAL SPEED, RPM

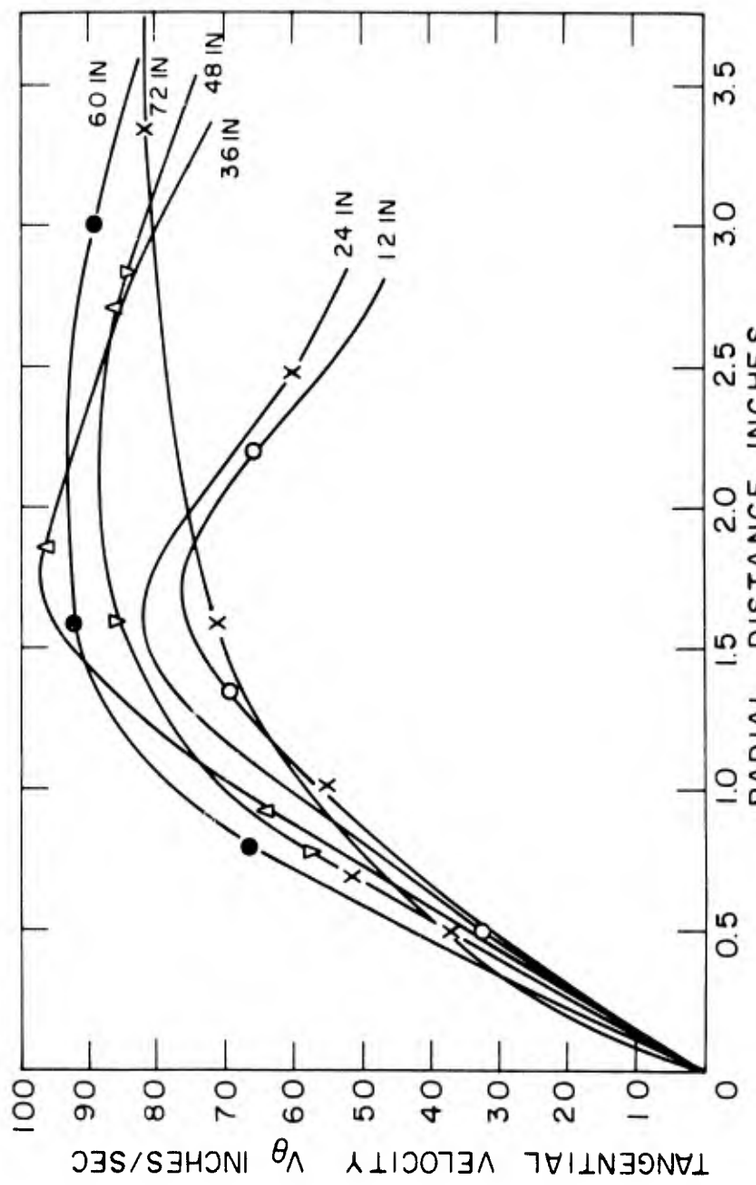

FIG. 5 TANGENTIAL VELOCITY VS. RADIAL DISTANCE, FROM TABLE I

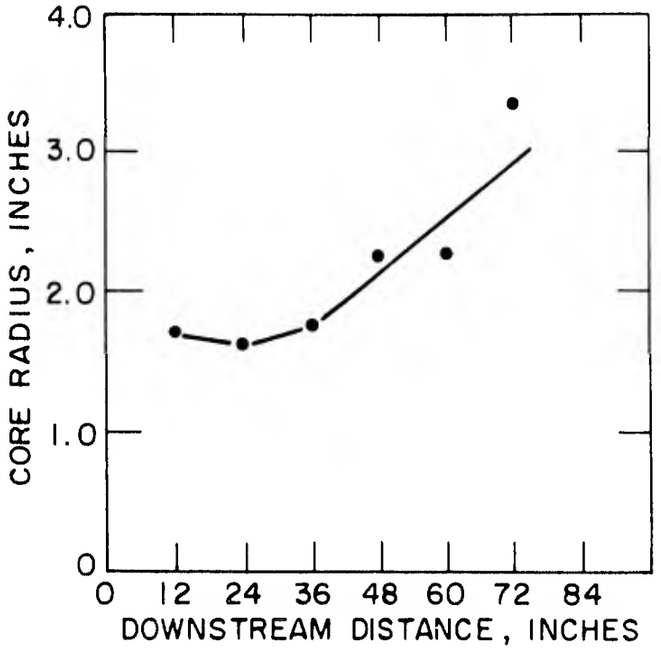

FIG. 6 CORE RADIUS VS. DOWNSTREAM DISTANCE, FROM FIGURE 10

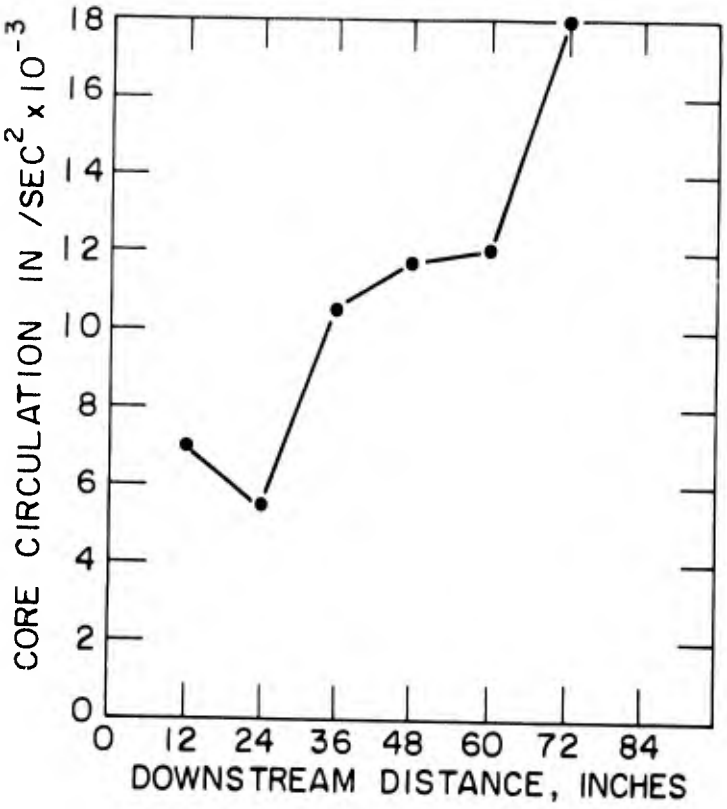

FIG. 7 CORE CIRCULATION VS. DOWNSTREAM DISTANCE, FROM TABLE II

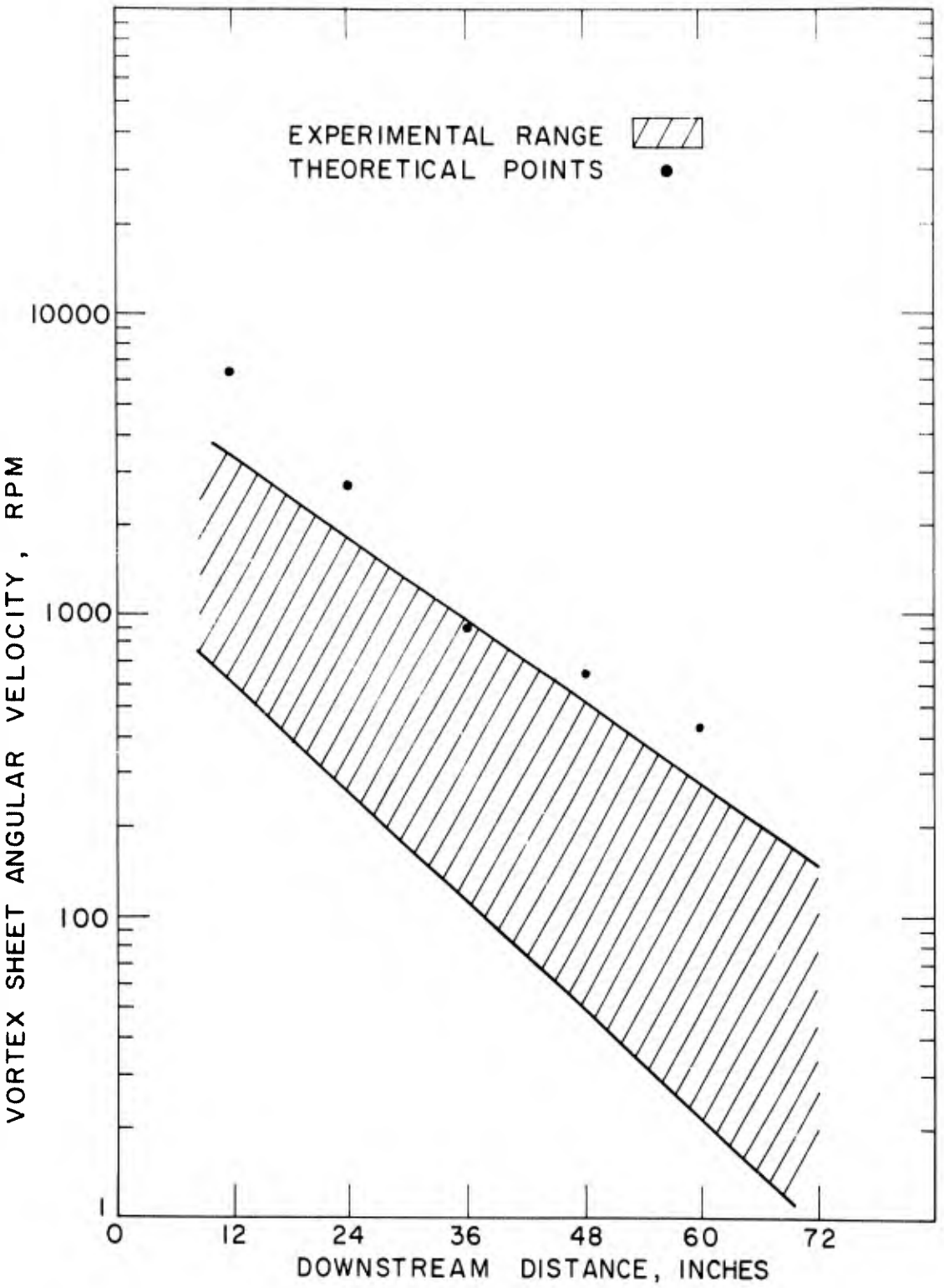

FIG. 8 COMPARISON OF SHEET ANGULAR VELOCITY : EXPERIMENT AND THEORY

Unclassified
Security Classification

DOCUMENT CONTROL DATA - R&D

(Security classification of title, body of abstract and indexing annotation must be entered when the overall report is classified)

1. ORIGINATING ACTIVITY *(Corporate author)*
Massachusetts Institute of Technology

2a. REPORT SECURITY CLASSIFICATION
Unclassified

2b GROUP
NA

3. REPORT TITLE
VORTEX WAKE ROLLUP AND VORTICITY CONCENTRATION BEHIND AN AIRFOIL

4. DESCRIPTIVE NOTES *(Type of report and inclusive dates)*
Technical Report

5. AUTHOR(S) *(Last name, first name, initial)*
McMahon, Thomas Arthur
Widnall, Sheila Evans

6. REPORT DATE	7a. TOTAL NO. OF PAGES	7b. NO. OF REFS
June 1967	26	3

8a. CONTRACT OR GRANT NO.	9a. ORIGINATOR'S REPORT NUMBER(S)
DA-31-124-ARO-D-471	ASRL TR 143-1
b. PROJECT NO. 20014501B33G	
c.	9b. OTHER REPORT NO(S) *(Any other numbers that may be assigned this report)*
d.	6495.1-E

10. AVAILABILITY/LIMITATION NOTICES
Distribution of this report is unlimited.

11. SUPPLEMENTARY NOTES	12. SPONSORING MILITARY ACTIVITY
None	U.S. Army Research Office-Durham Box CM, Duke Station Durham, North Carolina 27706

13. ABSTRACT Some important experimental evidence seems to confirm that the near wake problem is basically three-dimensional and should be reexamined as such. A concentration mechanism based on this three-dimensionality is proposed and found to predict a gradient of core circulation which is dimensionally correct and gives realistic answers when specific numerical cases are compared to published experiments. The correlation of experiment with theory involves a uniform translation of the theoretical points a specific distance upstream, implying that rotational fluid in the sheet requires a finite, uniform time to get to the core, no matter which downstream station we consider. A paradox in the role of viscosity in the concentrating mechanism is discussed.

14. KEY WORDS
near wake problem
vortex sheet
viscous vortex

DD FORM 1 JAN 64 1473

Unclassified
Security Classification